

General electromagnetic density of modes for a one-dimensional photonic crystal

C. H. Raymond Ooi, T. C. Au Yeung,* T. K. Lim, and C. H. Kam

School of Electrical and Electronic Engineering, Nanyang Technological University, Singapore 639798

(Received 29 October 1999; revised manuscript received 17 July 2000)

In this paper, we present more general, exact, and concise expressions for calculating the electromagnetic density of modes (EDOM) in one dimension photonic crystal (superlattice) for E and H polarizations. The expression is used for numerical computation of the EDOM in the lower-index (dielectric constant) layer. We discuss the difference between the EDOM in high- and low-index layers as due to the presence of waveguiding modes and evanescent-excited Bloch modes in the higher-index layer. Two methods of computation are presented to compute the EDOM in the lower-index layer. We suggest the possibility of using the EDOM to establish population inversion, which may be useful for higher-frequency lasers (e.g., x rays) and control any radiative processes. We also elaborate on the limitations of the results of Alvarado Rodriguez *et al.* as due to the approximation used in the evaluation of $\partial\omega/\partial k_{y,z}$ for $\nabla_k\omega$ and comment on the limitations of the one-dimensional EDOM expression of Bendickson *et al.*

PACS number(s): 42.70.Qs, 71.20.-b

I. INTRODUCTION

The spontaneous emission rate of atoms (via the Fermi's golden rule [1]) and the spectral density of the blackbody radiation [2] are directly affected by fluctuating vacuum fields (VF's). Since the *electromagnetic density of modes* (EDOM) characterizes the mode density of the VF's, knowledge of how to control the EDOM enables us to engineer the VF's and various quantum-mechanical processes which depend on it. In the last decade, periodic structures with one, two, and three dimensions [3] have been proposed and fabricated. These so-called photonic crystals exhibit photonic band gaps that can be used to modify the EDOM. A superlattice is the simplest form of such periodic structure. Analytical expression of EDOM for one-dimensional (1D) photonic crystal has been derived for normal-incidence waves [4], which adequately describes the spontaneous emission of photon in only one direction. In reality, the photon can be emitted any direction around 4π sr. Therefore, it is necessary to obtain an expression of the EDOM which considers all possible directions of photon emission, as in Ref. [5].

In this paper, we present more general, concise, and exact expressions for the EDOM in a lower dielectric constant layer of a step index superlattice. Thus the dispersion of the electromagnetic waves is described by the transcendental equation [6]. In Sec. II, we present the derivation of the EDOM without any approximation. We derive the exact expressions for $\partial\omega/\partial k_y$ and $\partial\omega/\partial k_z$, from which we obtain the necessary conditions where these expressions approximate to Eq. (19) in Ref. [5] for the δ -function superlattice model. In Sec. III, we discuss two numerical approaches and the necessary limit of numerical integration for the constant-frequency surface, which leads to the same final results. We also discuss the contribution of the evanescent-excited Bloch modes and the waveguiding modes to the EDOM in the higher-dielectric-constant layer, referred as layer 2. In Sec. IV, we present the computation results for the EDOM in

layer 1 and suggest the possibility of using a modified EDOM to facilitate population inversion.

II. ELECTROMAGNETIC DENSITY OF MODES

The k -space volume occupied by each wave vector point $V/(2\pi)^3$ is derived by discretizing the wave vector using the periodic boundary condition and taking the quantization volume V to infinity. The number of modes, δN , having frequencies from ω to $\omega + \delta\omega$ is

$$\begin{aligned}\delta N &= \rho(\omega) \delta\omega \\ &= [V/(2\pi)^3] \sum_n \int_{\text{all}, k(\omega_n)} d^3k \\ &= [V/(2\pi)^3] \sum_n \int_{\text{all}, k(\omega_n)} dk_n dS_n, \quad (1)\end{aligned}$$

where dS_n and dk_n are the infinitesimal area and thickness of the surface elements on a constant-frequency surface in k space, respectively, and n is the band index.

Using $(\partial\omega_{nk}/\partial k_n)\delta k_n = \delta\omega$ with $|\nabla_k\omega_{nk}| = \partial\omega_{nk}/\partial k_n$ and by taking $\delta\omega \rightarrow 0$, Eq. (1) becomes

$$\rho(\omega) = dN/d\omega = [V/(2\pi)^3] \sum_n \int_{\text{all}, k(\omega_n)} dS_n / |\nabla_k\omega_{nk}|. \quad (2)$$

If we confine the Bloch waves in 1D, i.e., normal to the superlattice, the only possible wave vectors corresponding to each ω are $+k_B$ and $-k_B$. So Eq. (1) becomes $\delta N = (L/2\pi) \sum_n \int_{\text{all}, k(\omega_n)} dk_B = \sum_n \int_{\text{all}, k(\omega_n)} (\partial k_B / \partial \omega) \delta\omega$ and we have $\rho(\omega) = (L/\pi) \partial k_B / \partial \omega$, as in Ref. [4]. In the 1D periodic structure (superlattice), the wave vector in the superlattice is $\mathbf{k} = (k_B, k_y, k_z)$ where k_B is the Bloch wave component and $\beta = \sqrt{k_y^2 + k_z^2}$ is the conserved tangential wave number. Therefore, $\mathbf{k} = (k_B, \beta \cos \varphi, \beta \sin \varphi)$, where φ is the azimuthal angle around the x axis. The group velocity is expressed as

*Email address: etcauyeung@ntu.edu.sg

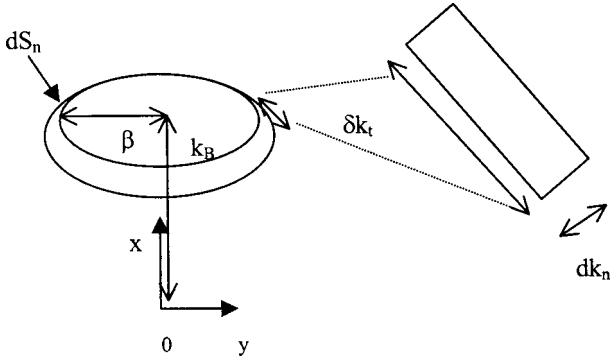


FIG. 1. Surface element of a constant-frequency surface for a superlattice.

$$\nabla_k \omega_{nk} = \left(\frac{\partial \omega_{nk}}{\partial k_B} \Big|_{\beta}, \frac{\partial \omega_{nk}}{\partial \beta} \Big|_{k_B}, \frac{\partial \omega_{nk}}{\partial k_y} \Big|_{k_B}, \frac{\partial \omega_{nk}}{\partial k_z} \Big|_{k_B} \right),$$

and the constant frequency surface element (Fig. 1) is $dS_n = 2\pi\beta dk_t$, where $\delta k_t = \delta\beta\sqrt{1 + (\delta k_B/\delta\beta)^2}$. From the transcendental equation (4), the variables k_B , ω , and β are mutually dependent, from which we have $\partial k_B/\partial\beta|_{\omega} = -(\partial\omega/\partial\beta|_{k_B})/(\partial\omega/\partial k_B|_{\beta})$. Therefore, $dS_n = 2\pi\beta d\beta [1 + (\partial\omega/\partial\beta|_{k_B})^2/(\partial\omega/\partial k_B|_{\beta})^2]^{1/2}$ and $|\nabla_k \omega_{nk}| = [(\partial\omega/\partial\beta|_{k_B})^2 + (\partial\omega/\partial k_B|_{\beta})^2]^{1/2}$. Using these relations, Eq. (2) is reduced to a more concise EDOM expression for each polarization,

$$\rho_i^p(\omega) = [V/(2\pi)^2] 2 \sum_n \int_0^{\sqrt{\varepsilon_i}\omega/c} \beta d\beta / (\partial\omega/\partial k_B|_{\beta}^p), \quad (3)$$

where the factor of 2 is due to the upper and lower parts of the constant-frequency surface, $i (= 1, 2)$ is the layer index, and $p (= E, H)$ is the polarization index.

By using Eq. (3), the computation of the EDOM is greatly simplified, since it is not necessary to evaluate the terms $\partial\omega/\partial k_y$ and $\partial\omega/\partial k_z$, as was done in Ref. [5]. We only need to evaluate $\partial\omega/\partial k_B|_{\beta}$ using the transcendental equations

$$\cos k_B a = [(\gamma + 1/\gamma + 2)\cos\alpha_+ - (\gamma + 1/\gamma - 2)\cos\alpha_-]/4, \quad (4a)$$

$$\cos k_B a = \cos\alpha_1 \cos\alpha_2 - \frac{1}{2}(\gamma + 1/\gamma)\sin\alpha_1 \sin\alpha_2, \quad (4b)$$

with $\alpha_{\pm} = \alpha_2 \pm \alpha_1$, $\alpha_i = k_{ix} d_i$, $k_{ix} = [(\omega/c)^2 \varepsilon_i - \beta^2]^{1/2}$, $\beta = (\omega/c)\sqrt{\varepsilon_i} \sin\theta_i$, $\gamma_e = k_{1x}/k_{2x}$, and $\gamma_h = \gamma_e(\varepsilon_2/\varepsilon_1)$, where d_i , ε_i , and θ_i are the thickness, dielectric constant, and wave vector angle, respectively, in layer $i (= 1, 2)$ of the superlattice, and $a = d_1 + d_2$ is the period or lattice constant.

Using Eq. (4a), we have the analytical expression of

$$\begin{aligned} \partial\omega/\partial k_B|_{\beta} = & 4a \sin k_B a / \{ [C \cos\alpha_+ - D_+ A_+ \sin\alpha_+] \\ & - [C \cos\alpha_- - D_- A_- \sin\alpha_-] \}, \end{aligned} \quad (5)$$

where $A_{\pm} = (\gamma + 1/\gamma \pm 2)$, $C = \partial A_{\pm}/\partial\omega$, and $D_{\pm} = \partial\alpha_{\pm}/\partial\omega$.

An alternate expression of the EDOM to Eq. (3) can be obtained by substituting $\beta(\omega, \theta_2) = \sqrt{\varepsilon_2}(\omega/c)\sin\theta_2$ (assuming $\varepsilon_2 > \varepsilon_1$) and converting the wave number summation to an angular summation,

$$\rho_i^p(\omega) = V(\omega/2\pi c)^2 \int_0^{\theta_{2,i}} \varepsilon_2 \sin 2\theta_2 d\theta_2 / (\partial\omega/\partial k_B|_{\beta}^p), \quad (6)$$

where $\theta_{2,i} = \sin^{-1}\sqrt{\varepsilon_i/\varepsilon_2}$ and $\partial\omega/\partial k_B|_{\beta}^p$ now depends explicitly on θ_2 instead of β .

The gradient of the band structure $1/\partial k_B/\partial\omega|_{\theta_2}$ is related to $\partial\omega/\partial k_B|_{\beta}$ by

$$\begin{aligned} \partial\omega/\partial k_B|_{\beta} = & 1/[\partial k_B/\partial\omega|_{\theta_2} - (\partial k_B/\partial\theta_2|_{\omega}) \\ & \times (\partial\beta/\partial\omega|_{\theta_2})/(\partial\beta/\partial\theta_2|_{\omega})] \\ = & 1/[\partial k_B/\partial\omega|_{\theta_2} - (\partial k_B/\partial\theta_2|_{\omega} \tan\theta_2/\omega)]. \end{aligned} \quad (7)$$

In the final part of this section, we use Eq. (4b) to derive the dispersion relation for the δ -function superlattice [5] and obtain exact expressions for $\partial\omega/\partial k_y$ and $\partial\omega/\partial k_z$. The δ -function model defines that the higher-index layer has a dielectric constant $\varepsilon_2 (\gg \varepsilon_1)$ and infinitesimal thickness of $d_2 (\ll a)$, such that $d_1 \approx a$, $\alpha_2 \ll \pi/2$, $\alpha_1 \approx k_{1x}a$, and Eq. (4b) reduces to

$$\cos k_B a = \cos k_{1x} a - \Omega \sin k_{1x} a, \quad (8)$$

where $\Omega = g a \omega^2 / 2c^2 k_{1x}$ and $g = (\varepsilon_2 - \varepsilon_1)d_2/a$ is the grating strength [5].

The necessary conditions for Eq. (8) to be valid are

$$(a) \quad d_2(\omega/c)\sqrt{\varepsilon_2} \ll \pi/2 \quad \text{or} \quad 1 - r \ll 1/(4y\sqrt{\varepsilon_2}) \quad (9a)$$

and

$$(b) \quad 2k_{1x}^2 \ll (\omega/c)^2(\varepsilon_2 - \varepsilon_1) \quad \text{or} \quad \varepsilon_2 \gg 3\varepsilon_1, \quad (9b)$$

where $y = \omega a / 2\pi c$ is the dimensionless frequency and $r = d_1/a$ is the dimensionless thickness of layer 1 by setting $\varepsilon_2 > \varepsilon_1$.

The exact expressions of $\partial\omega/\partial k_y$ and $\partial\omega/\partial k_z$ for the δ -function model can be obtained by differentiating Eq. (8) with respect to k_y ,

$$\begin{aligned} \frac{\partial\omega}{\partial k_y} = & \frac{c^2 k_y}{\omega \varepsilon_1} \frac{[\sin k_{1x} a + \Omega(\cos k_{1x} a - \sin k_{1x} a)]}{[(1 + g/\varepsilon_1)\sin(k_{1x} a) + \Omega(\cos k_{1x} a - \sin k_{1x} a)]}. \end{aligned} \quad (10)$$

Exactly the same form of expression is obtained for $\partial\omega/\partial k_z$.

We only have the approximation of $\partial\omega/\partial k_y \approx c^2 k_y / \omega \varepsilon_1$ and $\partial\omega/\partial k_z \approx c^2 k_z / \omega \varepsilon_1$ [as in Eq. (27) of Ref. [5]] when the difference between the bracketed numerator and denominator of Eq. (10) is much smaller than the bracketed numerator, i.e.,

$$\begin{aligned} D = & |(1 + g/\varepsilon_1)\sin k_{1x} a + \Omega(\cos k_{1x} a - \sin k_{1x} a)| \\ & - (g/\varepsilon_1)|\sin k_{1x} a| \gg 0. \end{aligned} \quad (11)$$

Since Ω and k_{1x} depend explicitly on frequency and propagation angle through k_y and k_z , the approximation yields good EDOM results only when condition (11) is satisfied for all possible propagation angles for a specific frequency and structural parameters d_i/a and ε_i . If D is close to zero or negative, condition (11) is not satisfied and the approximation becomes invalid.

III. COMPUTATION OF THE EDOM

Equation (3) can be evaluated numerically by wave number β summation for each frequency point ω . Any propagating mode that can be created at a particular space point in the superlattice will contribute to the EDOM at that point. Thus the summation range of $\beta=0 \rightarrow (\omega/c)$ corresponds to the propagating Bloch modes with real k_{1x} , k_{2x} , and k_B that can be created by a radiative source from outside as well as inside the superlattice. The summation range of $\beta=(\omega/c) \rightarrow (\omega/c)\sqrt{\varepsilon_1}$ also corresponds to real k_{1x} , k_{2x} , and k_B , but can only be excited from within the superlattice. The summation range of $\beta=(\omega/c)\sqrt{\varepsilon_1} - (\omega/c)\sqrt{\varepsilon_2}$ corresponds to modes with imaginary k_{1x} and real k_{2x} . However, k_B is real only for a frequency below a certain threshold, which can also be excited by the evanescent fields in layer 1. Beyond this threshold, k_B becomes imaginary since the evanescent fields in layer 1 decay too rapidly and cannot excite the Bloch modes. Here the fields from two adjacent layers 2 do not couple. The electromagnetic fields within layer 2 undergo repeated total internal reflection. The propagating Bloch modes become waveguide modes. These modes contribute to the EDOM of layer 2 only. The modes corresponding to imaginary k_{1x} can only be excited in the higher-index layer (layer 2) and not in layer 1, and therefore do not contribute to the EDOM of layer 1. Thus the EDOM for layers 1 and 2 require the overall summation range of $\beta=0 \rightarrow (\omega/c)\sqrt{\varepsilon_1}$ and $\beta \rightarrow (\omega/c)\sqrt{\varepsilon_2}$, respectively, for $\varepsilon_2 > \varepsilon_1$. In this paper, we discuss the results for the EDOM in layer 1 only.

In the limit $\varepsilon_2 - \varepsilon_1 \rightarrow 0$, where the superlattice becomes a homogeneous medium, we show that Eq. (4a) still gives correct results. The constant-frequency surface becomes spherical and dispersionless. From Eq. (4a), we have $k_B \approx k_{1x} \approx k_{2x} = k_x = \sqrt{\varepsilon}(\omega/c)\cos\theta_m$, while the tangential component remains as $\beta = \sqrt{\varepsilon}(\omega/c)\sin\theta_m$. By differentiation of $\varepsilon(\omega/c)^2 = k_B^2 + \beta^2$, we have $\partial\omega/\partial k_B|_{\beta} = (c \cos\theta_m)/\sqrt{\varepsilon}$, $\partial\omega/\partial\beta|_{k_B} = (c \sin\theta_m)/\sqrt{\varepsilon}$, and the group velocity is $|\nabla_k \omega_{nk}| = c/\sqrt{\varepsilon}$, with wave vector $\mathbf{k} = (k_B, \beta)$. By substituting $\partial\omega/\partial k_B|_{\beta}$ into Eq. (6), we have the EDOM for a homogeneous medium,

$$\rho(\omega) = V\varepsilon^{3/2}\omega^2/2\pi^2c^3. \quad (12)$$

We observe that the EDOM is enhanced in a high dielectric medium. In free space, Eq. (12) reduces to $\rho_0(\omega) = V\omega^2/2\pi^2c^3$ for each polarization.

IV. RESULTS AND DISCUSSION

Figures 2–4 show the plot of dimensionless frequency $\omega a/2\pi c$ versus EDOM (arbitrary scale) for layer 1 (lower dielectric constant) of the superlattice. The numerical inte-

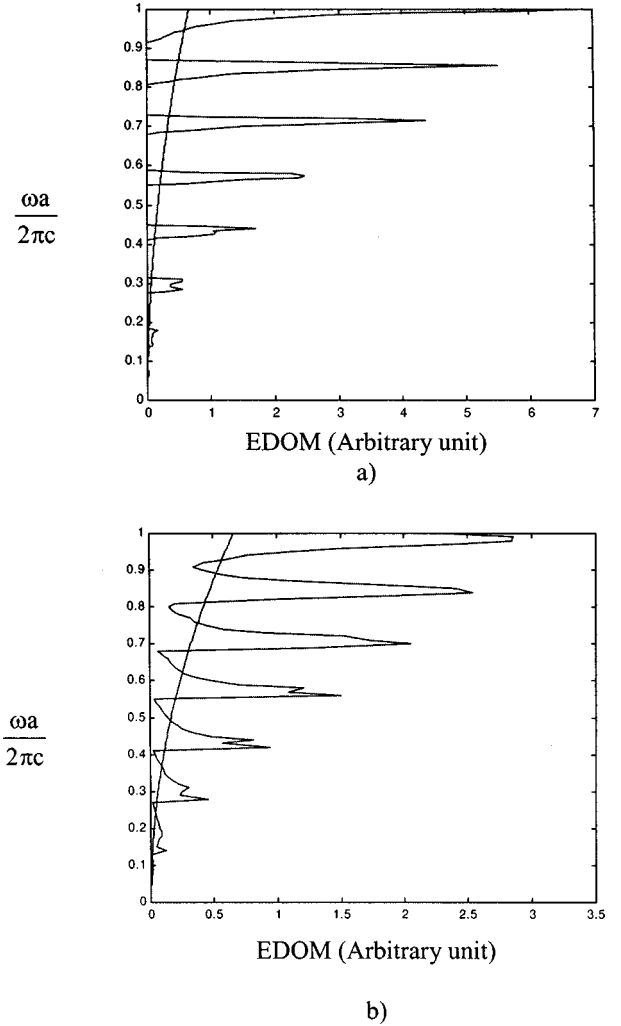


FIG. 2. Dimensionless frequency versus EDOM with extremely high index contrast $\varepsilon_1=1$, $\varepsilon_2=50$, and $r=0.5$, for (a) E polarization and (b) H polarization. The solid line shows the EDOM for unpolarized light in a vacuum.

gration results obtained from Eq. (3) by wave number summation and from Eq. (6) by angular summation are exactly the same. However, the angular summation approach requires less computation time due to the constant upper limit of the integration.

Figures 2(a) and 2(b) show the existence of high-contrast EDOM profiles (with sharp peaks, each resembles the Dirac δ function) for the case of extremely high dielectric contrast between layers 1 and 2. For E polarization [see Fig. 2(a)] the EDOM vanishes at certain ranges of frequencies, called EDOM gaps. These gaps are useful for the suppression of the spontaneous emission of atoms located in layer 1, while the sharp peaks (similar to Van Hove singularities) are useful for spontaneous emission enhancement. The EDOM gap exists at the lower-frequency region only. As the frequency increases, the gap becomes smaller and vanishes. For H polarization [see Fig. 2(b)] we hardly observe any EDOM gap of finite size for any choice of parameters. The EDOM drops very steeply to near zero at the lower-frequency side of the Van Hove peaks, with gradient $\partial\rho/\partial\omega$ approaching infinity. This feature is very useful since the gradient can be made extremely steep by using extremely high-dielectric-constant

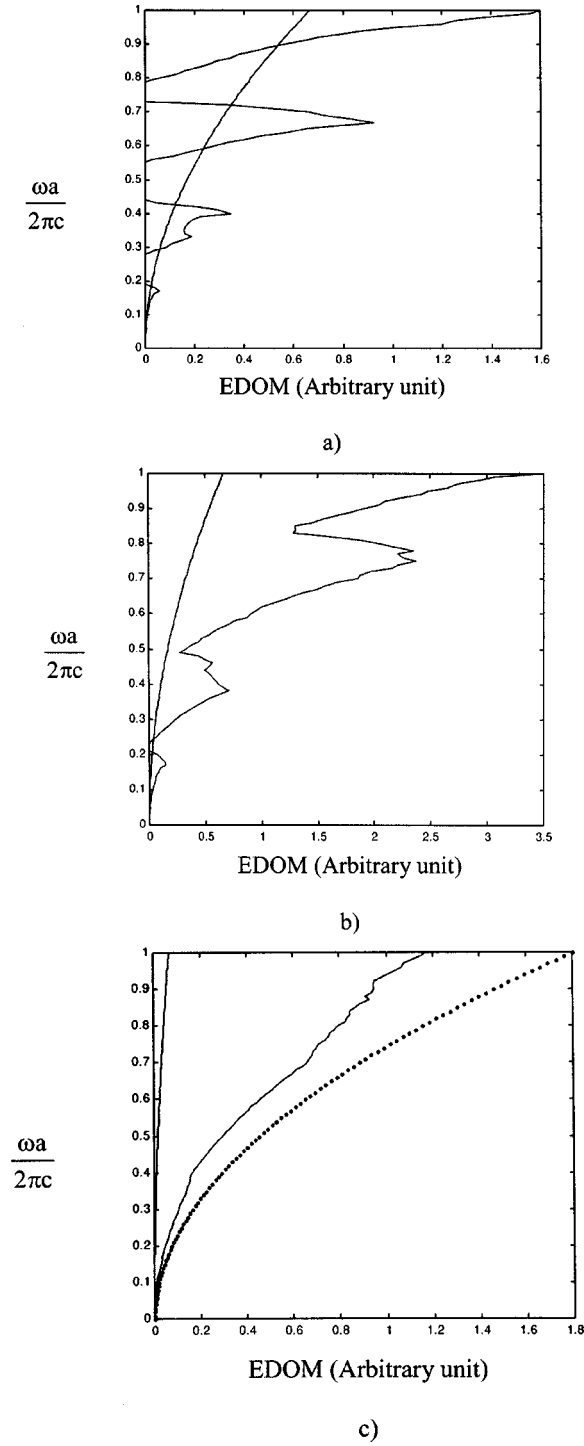


FIG. 3. Dimensionless frequency versus EDOM for E polarization with index contrast of (a) high contrast, $\epsilon_1=1, \epsilon_2=10$, and $r=0.5$, (b) medium contrast, $\epsilon_1=3, \epsilon_2=10$, and $r=0.5$, and (c) low contrast, $\epsilon_1=8, \epsilon_2=10$, and $r=0.5$ superimposed with the vacuum EDOM (solid line) and averaged medium EDOM (dotted line) [from Eq. (12)] for unpolarized light.

ϵ_2 material in layer 2, such as ferroelectrics [7]. Another interesting feature of Figs. 2(a) and 2(b) is the constant spacing between adjacent peaks.

For an example of practical application, we consider two hyperfine splitted energy levels E_d and E_u which spontaneously emit photons of frequencies ω_d and $\omega_u = \omega_d + \Delta\omega$, respectively, when relaxing to a common ground level E_g .

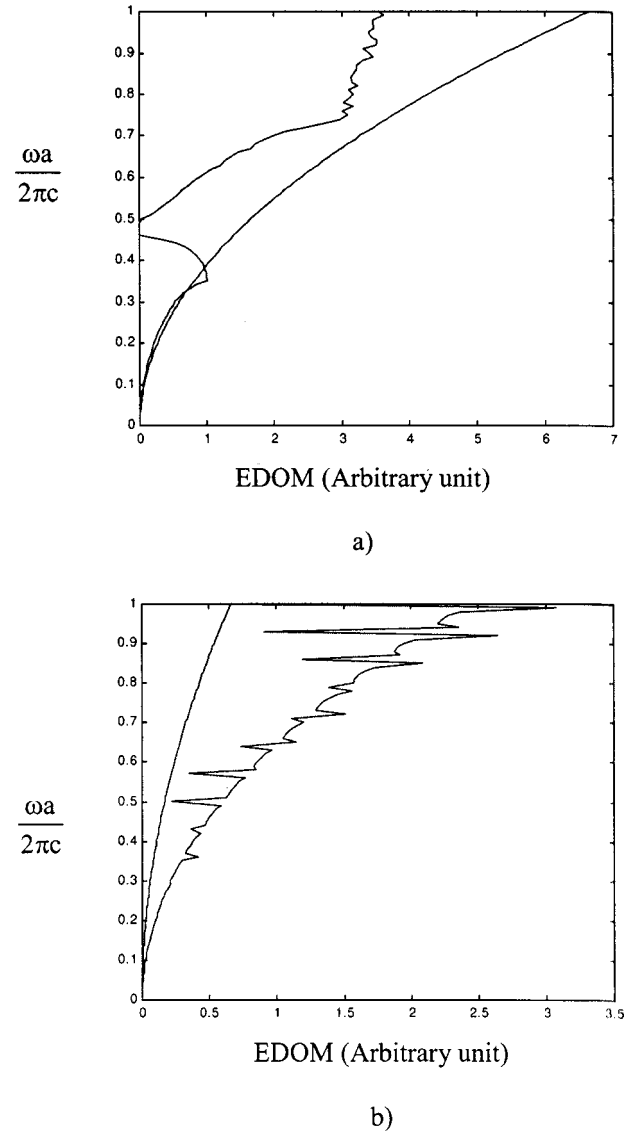


FIG. 4. Dimensionless frequency versus EDOM for E polarization with (a) high index in an extremely narrow layer, $\epsilon_1=1, \epsilon_2=50$, and $r=0.99$, and (b) high index in an extremely thick layer, $\epsilon_1=1, \epsilon_2=50$, and $r=0.01$. The solid line shows the vacuum EDOM for unpolarized light.

The frequencies ω_d and ω_u can be made to coincide with the EDOM peak and EDOM gap edge, respectively. By doing so, the E_d level which corresponds to a very high EDOM becomes lowly populated, while E_u becomes highly populated, thus creating a population inversion. The transition $E_u \rightarrow E_d$ can be triggered by either *eliminating* or *reversing* the EDOM contrast between the two levels. This can be done, for example, by electrically tuning the dielectric constant of one of the layers. Thus coherent emission of photons at any frequency corresponding to two energy levels can be created. The periodic structure provides a way of using the hyperfine-split energy levels for ultralow-frequency lasers as well as very large electronic band gaps for higher-frequency (e.g., x-ray) lasers. In principle, an engineered EDOM can be used to control essentially any radiative-transition process, ranging from the transition in molecular rotational energy to nuclear hyperfine transitions.

Figures 3(a)–3(c) show that as the dielectric contrast

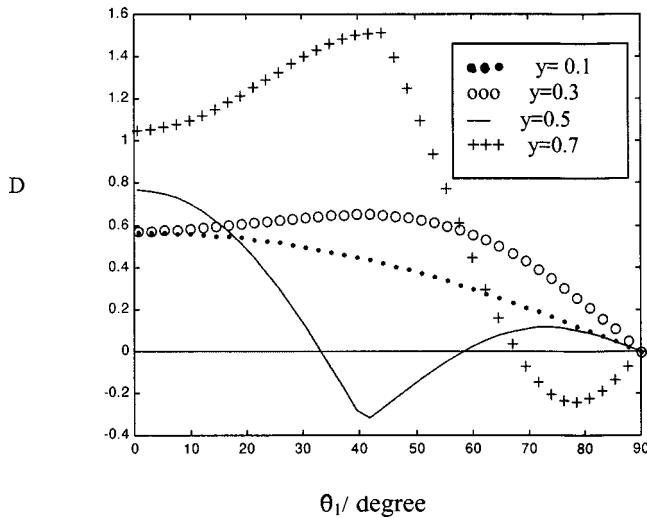


FIG. 5. Analysis for valid approximation for a δ function model [Fig. 4(a), D [condition (11)] versus θ_1 , the incidence angle in layer 1, for several values of y ($=\omega a/2\pi c$).

($\varepsilon_2 - \varepsilon_1$) reduce, the EDOM profile becomes smoother and nearer to the effective homogeneous medium profile, with less peak-valley contrast and a nonzero EDOM for all frequencies. For comparison, the homogeneous medium EDOM, Eq. (12), is only superimposed in Fig. 2(c) where the dielectric contrast is small and ε assumes the effective dielectric constant, $\varepsilon_1 r + \varepsilon_2(1-r)$.

We observe that Figs. 4(a) and 4(b) (with very large $\varepsilon_2 - \varepsilon_1$ and extreme values of r) hardly display many EDOM gaps. Thus the combination of large dielectric contrast ($\varepsilon_2 - \varepsilon_1$) and moderate layer ratio thickness (r) is necessary for creating the EDOM gaps. The EDOM of Fig. 4(a) corre-

sponds to the δ -function superlattice, as modeled in Ref. [5], since it has the structure parameters that satisfy condition (9) for ($y = \omega a/2\pi c$) $\ll 3.54$ and with a grating strength of $g = 0.49$ [Eq. (8)]. As such, the EDOM profile of Fig. 4(a) should closely match that of Fig. 5 in Ref. [5]. In fact, it does for $\omega a/2\pi c$ below about 0.4, except for the EDOM dip (gap) at around $\omega a/2\pi c \approx 0.5$ [see Fig. 4(a)], which is not found in Fig. 5 of [5]. This is because the necessary condition (11) for the approximation is not satisfied. This can be verified by plotting D from condition (11) versus θ_1 (see Fig. 5), where we have used $k_{ix} = (\omega/c)\sqrt{\varepsilon_1}\cos\theta_1$. In the vicinity of $\omega a/2\pi c \approx 0.5$, we have a wide range of θ_1 where D is negative, i.e., when the approximation is invalid. However, for $y < 0.4$, the approximation is good, and D is positive for any angle of incidence. Figure 4(b) shows the EDOM with an equally spaced ‘‘abyss’’ for a superlattice with the structure which complements that of the δ -function superlattice of Fig. 4(a).

V. CONCLUSION

We have presented general, exact, and more concise expressions for calculating the EDOM in a lower-index layer of a one-dimension photonic crystal (superlattice) for both E and H polarizations. The expression [Eq. (6)] has been used to compute the EDOM in the lower-index layer. We suggested the possibility of using an engineered EDOM to establish population inversion and to control essentially any radiative process, with the potential usage in extreme frequency lasers. We have derived the dispersion relation for the δ -function superlattice of Ref. [5]. We have also quantitatively explained and analyzed the differences and similarities between our results [Figs. 4(a) and 5] and that of Ref. [5] (Fig. 5 therein).

[1] H. Yokoyama and K. Ujihara, *Spontaneous Emission and Laser Oscillation in Microcavities* (CRC, New York, 1995).
 [2] P. W. Milonni, *The Quantum Vacuum: An Introduction to Quantum Electrodynamics* (Academic, San Diego, 1994).
 [3] E. Yablonovitch, Phys. Rev. Lett. **58**, 2059 (1987).
 [4] Jon M. Bendickson, Jonathan P. Dowling, and Michael Scalora, Phys. Rev. E **53**, 4107 (1996).

[5] I. Alvarado Rodriguez, P. Halevi, and J. J. Sanchez-Mondragon, Phys. Rev. E **59**, 3624 (1999).
 [6] P. Yeh, *Optical Waves in Layered Media* (Wiley, New York, 1988).
 [7] C. Kittel, *Introduction to Solid State Physics* (Wiley, New York, 1986).